68. Flory, P. J. *Principles of Polymer Chemistry* (Cornell University Press, New York, 1953).
69. Wang, L-L. & Bryan, J. *Cell* **25,** 637–649 (1981).
70. Yin, H. L., Maruyama, K. & Stossel, T. P. *J. biol. Chem.* **256,** 9693–9697 (1981).
71. Chaponnier, C., Borgia, R., Rungger-Brandle, E., Weil, R. & Gabbiani, C. *Experientia* **35,** 1039–1041 (1979).
72. Norberg, R., Thorstensson, R., Utter, G. & Fragraeus, A. *Aur. J. Biochem.* **100,** 575–583 (1979).
73. Harris, H. E., Bamburg, J. R. & Weeds, A. G. *FEBS Lett.* **121,** 175–177 (1980).
74. Harris, H. E. & Gooch, J. *FEBS Lett.* **123,** 49–53 (1981).
75. Harris, D. A. & Schwartz, J. H. *Proc. natn. Acad. Sci. U.S.A.* **78,** 6798–6802 (1981).
76. Yin, H. L., Albrecht, J. H. & Fattoum, A. *J. Cell Biol.* **91,** 901–906 (1981).
77. Harris, H. E., Bamburg, J. R., Bernstein, B. W. & Weeds, A. G. *Analyt. Biochem.* **119,** 102–114 (1982).
78. Hasegawa, T., Takahashi, S., Hayashi, H. & Hatano, S. *Biochemistry* **19,** 2677–2683 (1980).
79. Hinssen, H. *Eur. J. Cell Biol.* **23,** 225–233 (1981).
80. Hinssen, H. *Eur. J. Cell Biol.* **23,** 234–240 (1981).
81. Brown, S. S., Yamamoto, K. & Spudich, J. A. *J. Cell Biol.* (in the press).
82. Isenberg, G., Aebi, U. & Pollard, T. D. *Nature* **288,** 455–459 (1980).
83. Bamburg, J. R., Harris, H. E. & Weeds, A. G. *FEBS Lett.* **121,** 178–182 (1980).
84. Mooseker, M. S. & Tilney, L. G. *J. Cell Biol.* **67,** 725–743 (1975).
85. Matsudaira, P. T. & Burgess, D. R. *J. Cell Biol.* **83,** 667–673 (1979).
86. Howe, C. L., Mooseker, M. S. & Graves, T. A. *J. Cell Biol.* **86,** 916–923 (1980).
87. Glenney, J. R., Bretscher, A. & Weber, K. *Proc. natn. Acad. Sci. U.S.A.* **77,** 6458–6462 (1980).
88. Bretscher, A. & Weber, K. *Proc. natn. Acad. Sci. U.S.A.* **76,** 2321–2325 (1979).
89. Bretscher, A. & Weber, K. *Cell* **20,** 839–847 (1980).
90. Glenney, J. R., Kaulfus, P. & Weber, K. *Cell* **24,** 471–480 (1981).
91. Craig, S. W. & Powell, L. D. *Cell* **22,** 739–746 (1980).
92. Mooseker, M. S., Graves, T. A., Wharton, K. A., Falco, N. & Howe, C. L. *J. Cell Biol.* **87,** 809–822 (1980).
93. Matsudaira, P. T. & Burgess, D. R. *J. Cell Biol.* (in the press).
94. Glenney, J. R. & Weber, K. *Proc. natn. Acad. Sci. U.S.A.* **78,** 2810–2814 (1981).
95. Glenney, J. R., Geisler, N., Kaulfus, P. & Weber, K. *J. biol. Chem.* **256,** 8156–8161 (1981).
96. Drenckhahn, D. & Groschel-Stewart, U. *J. Cell Biol.* **86,** 475–482 (1980).
97. Herman, I-M. & Pollard, T. D. *J. Cell Biol.* **88,** 346–351 (1981).
98. Kendrick-Jones, J. & Scholey, J. *J. Muscle Res. Cell Motility* **2,** 347–372 (1981).
99. Stossel, T. P., Hartwig, J. H., Yin, H. L., Zaner, K. S. & Stendahl, O. *Cold Spring Harb. Symp. quant. Biol.* **46** (in the press).
100. Tilney, L. G., Binder, E. M. & DeRosier, D. J. *J. Cell Biol.* **90,** 485–494 (1981).
101. Tilney, L. G., Hatano, S., Ishikawa, H. & Mooseker, M. S. *J. Cell Biol.* **59,** 109–126 (1973).
102. Tilney, L. G., Kiehart, D. P., Sardet, C. & Tilney, M. *J. Cell Biol.* **77,** 536–550 (1978).
103. Carlsson, L., Markey, F., Blikstad, I., Persson, T. & Lindberg, U. *Proc. natn. Acad. Sci. U.S.A.* **76,** 6376–6380 (1979).
104. Casella, J. F., Flanagan, M. D. & Lin, S. *Nature* **293,** 302–305 (1981).
105. Taylor, D. L. & Wang, Y-L. *Nature* **284,** 405–410 (1980).

ARTICLES

UV radiation from the young Sun and oxygen and ozone levels in the prebiological palaeoatmosphere

V. M. Canuto*, J. S. Levine†, T. R. Augustsson† & C. L. Imhoff‡

* NASA, Goddard Institute for Space Studies, New York, New York 10025, USA
† NASA, Langley Research Center, Hampton, Virginia 23665, USA
‡ C.S.C., NASA, Goddard Space Flight Center, Greenbelt, Maryland 20771, USA

UV measurements of young T-Tauri stars, resembling the Sun at an age of a few million years, have recently been made with the International Ultraviolet Explorer. They indicate that young stars emit up to 10^4 times more UV than the present Sun. The implications for the origin and evolution of O_2 and O_3 in the prebiological palaeoatmosphere are presented here. The results of photochemical calculations indicate that the O_2 surface mixing ratio was a factor 10^4–10^6 times greater than the standard value of 10^{-15}. This new value reconciles the simultaneous existence of oxidized iron and reduced uranium.

A RELIABLE picture of the environment of the early Earth depends critically on the correct quantification of the amount of solar radiation impinging on the Earth. Standard stellar evolutionary models predict that 4,500 Myr ago, the Sun's luminosity was lower than today by ~30% (ref. 1). This has created the 'dim Sun paradox' because such dimming translates into a decrease of the Earth's effective temperature, T_*, of ~8%, sufficient to keep T_* below the freezing point of seawater for ~2,000 Myr (ref. 2). On the other hand, there is evidence of liquid water as early as 3,500 Myr ago[2], so a paradox arises. Explanations proposed to solve the problem include either increasing the greenhouse efficiency[2–4] or varying the Earth's early albedo[5]. In either case, one makes inferences about the physical parameters characterizing the palaeoatmosphere using astronomical data.

We consider here another astronomical input, the UV radiation from the Sun which had a great impact on the early atmosphere of the Earth[6–12]. In fact, UV radiation initiated the photochemical processes that led to the formation of oxygen (O_2) and ozone (O_3) in the prebiological palaeoatmosphere. By virtue of its strong absorption in the UV (200–300 nm), ozone protects life at the surface of the Earth from this lethal radiation. Hence, the evolution of ozone, and its variation over geological time had very important implications for the biological evolution of primitive organisms[6–12]. An accurate quantification of the levels of oxygen and ozone in the prebiological

Table 1 Ratios of stellar to solar UV line fluxes intercepted at the distance of the Earth

λ(A)	Identity	T Tau	DR Tau	RW Aur	GW Ori	CoD-35°10525	RU Lup	S CrA
1,240	N V	2.5×10^5		$<4.0\times10^3$	2.3×10^5	6.1×10^4	2.4×10^3	
1,304	O I, Si II	1.3×10^5		9.4×10^3	9.9×10^4	3.0×10^4	6.5×10^3	
1,335	C II	7.8×10^4		9.6×10^2	4.3×10^4	1.7×10^4	1.9×10^4	
1,400	Si IV	2.2×10^5	5.5×10^4	1.2×10^4	2.3×10^5	2.0×10^4	3.3×10^4	2.4×10^4
1,550	C IV	1.4×10^5	8.8×10^4	3.2×10^3	1.5×10^5	2.9×10^4	1.2×10^4	8.1×10^3
1,640	He II	1.4×10^5	5.9×10^4	$\leq1.5\times10^3$	2.0×10^5	2.6×10^4	5.8×10^3	$\leq7.7\times10^3$
1,813	Si II, S I	2.9×10^4	1.9×10^4		1.1×10^4	2.8×10^3	5.1×10^3	5.6×10^3

The radii of the stars have been taken as (in solar radii): 6.8, 4.7, 3.1, 8.4, 3.4, 2.6, and 3.2, respectively.

0028–0836/82/170716—05$01.00

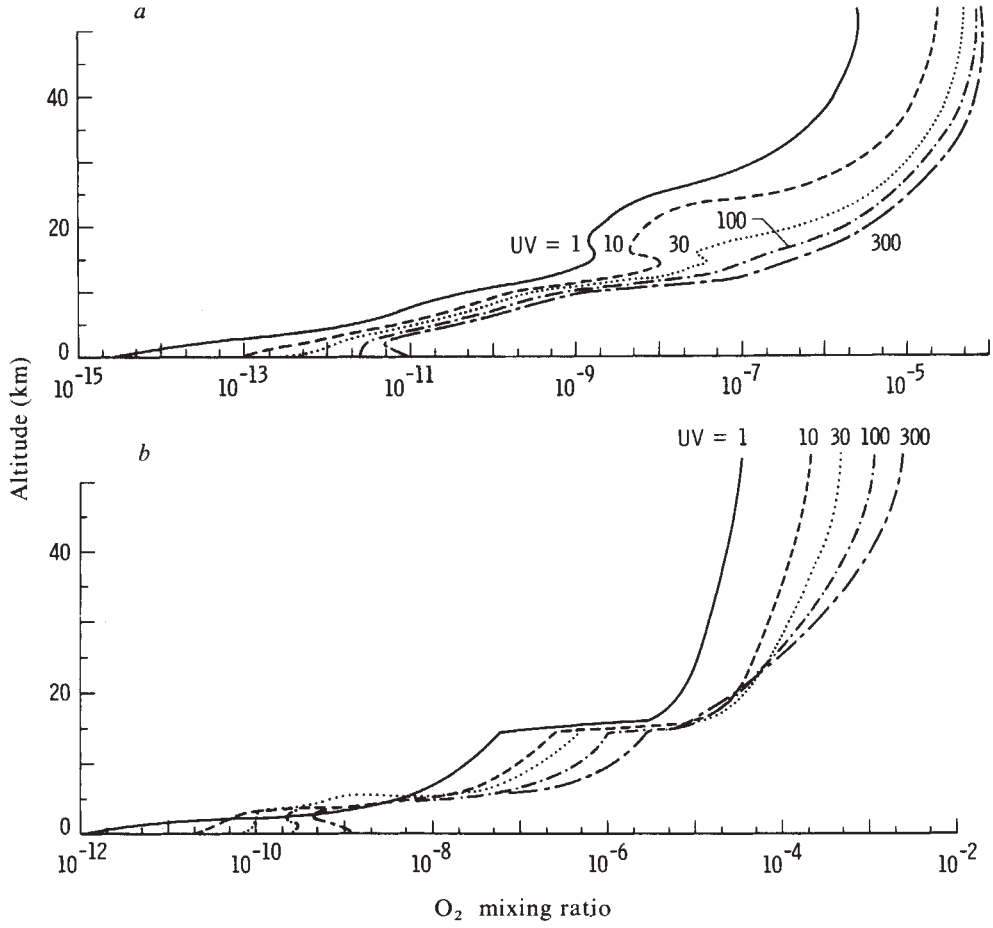

Fig. 1 Vertical distribution of O_2 in the prebiological palaeoatmosphere for levels of solar UV from 1 to 300 times the present value for a CO_2 level of: *a*, 280 p.p.m.v.; *b*, 28,000 p.p.m.v.

palaeoatmosphere and the level of UV radiation reaching the surface of the Earth are therefore important when considering biological evolution on Earth.

The stellar evolutionary models cannot be used to predict the amount of UV generated by the young Sun and one must, therefore, rely on direct observational data. Because until recently such data were available only for the present Sun, estimates for the past UV radiation were based either on the assumption that the lower solar luminosity also implied a lower UV component or else it was assumed that the UV radiation was the same in the past as it is today[6–12].

Recent observational data gathered through the International Ultraviolet Explorer (IUE) have, however, indicated that neither approach is correct. Young stars have been found to emit considerably more UV radiation than the present Sun.

The T-Tauri stars are very young stars with masses roughly equal to the Sun's. As such, they are considered to resemble the Sun at an age of a few million years. Several T-Tauri stars have recently been studied in the UV with IUE[13–17]. The primary result of these observations is that the stars emit strongly in the UV. Most noticeable are the chromospheric emission lines arising from the hot (10^4–10^5 K) atmospheres of the stars. The surface fluxes of the lines, (defined to be the flux emitted per unit stellar surface area), have been determined to be 100–5,000 times greater among the T-Tauri stars than in the Sun[18]. In addition, these protostars are still contracting and thus are larger than the Sun. Thus, the UV flux intercepted at the distance of the Earth is increased by an additional factor of $(R_*/R_\odot)^2$ due to the greater surface area of the protostar. We have computed the ratio of stellar-to-solar UV flux as would be measured at the Earth's distance for seven T-Tauri stars, given in Table 1. Radii for these stars were estimated from temperatures and luminosities of the stars largely taken from ref. 19. The values range from 3 to 8 solar radii and are given in Table 1. We find that the UV line flux from the T-Tauri stars is 10^3–10^4 times the present solar value.

The emission lines dominate the spectrum between 100 and 200 nm. At longer wavelengths the UV continuum of the T-Tauri stars dominates. The continuum fluxes are also enhanced by a few hundred times relative to the Sun. As we will discuss below, the wavelength intervals discussed here cover the maximum in the UV absorption cross-section of H_2O, CO_2, O_2, and O_3.

Young stars which are older than the T-Tauri stars continue to emit strongly in the UV, although not at the extreme levels of the T-Tauri stars. UV emission-line surface fluxes decrease with age approximately as $t^{-0.5}$ to $t^{-0.9}$ (ref. 20). The age dependence for the UV surface fluxes resembles that of Ca II emission, determined previously by ground-based near-UV observations[22–23]. We have computed the enhancement of the UV flux intercepted at the distance of the Earth as a function of age for a solar-type star, using the observational relationship reported in ref. 20 corrected for the changing radius of the contracting star. Radii at specific ages for solar mass stars were estimated from temperatures and luminosities in theoretical H–R diagrams[19]. The results are given in Table 2. We find that, even after the star has reached the main sequence (5×10^7 yr), begins

Table 2 Stellar UV flux as a function of age

Age (yr)	UV enhancement
10^6	10^4
10^7	500
5×10^7	100
10^8	32
5×10^8	8
10^9	4
5×10^9	1

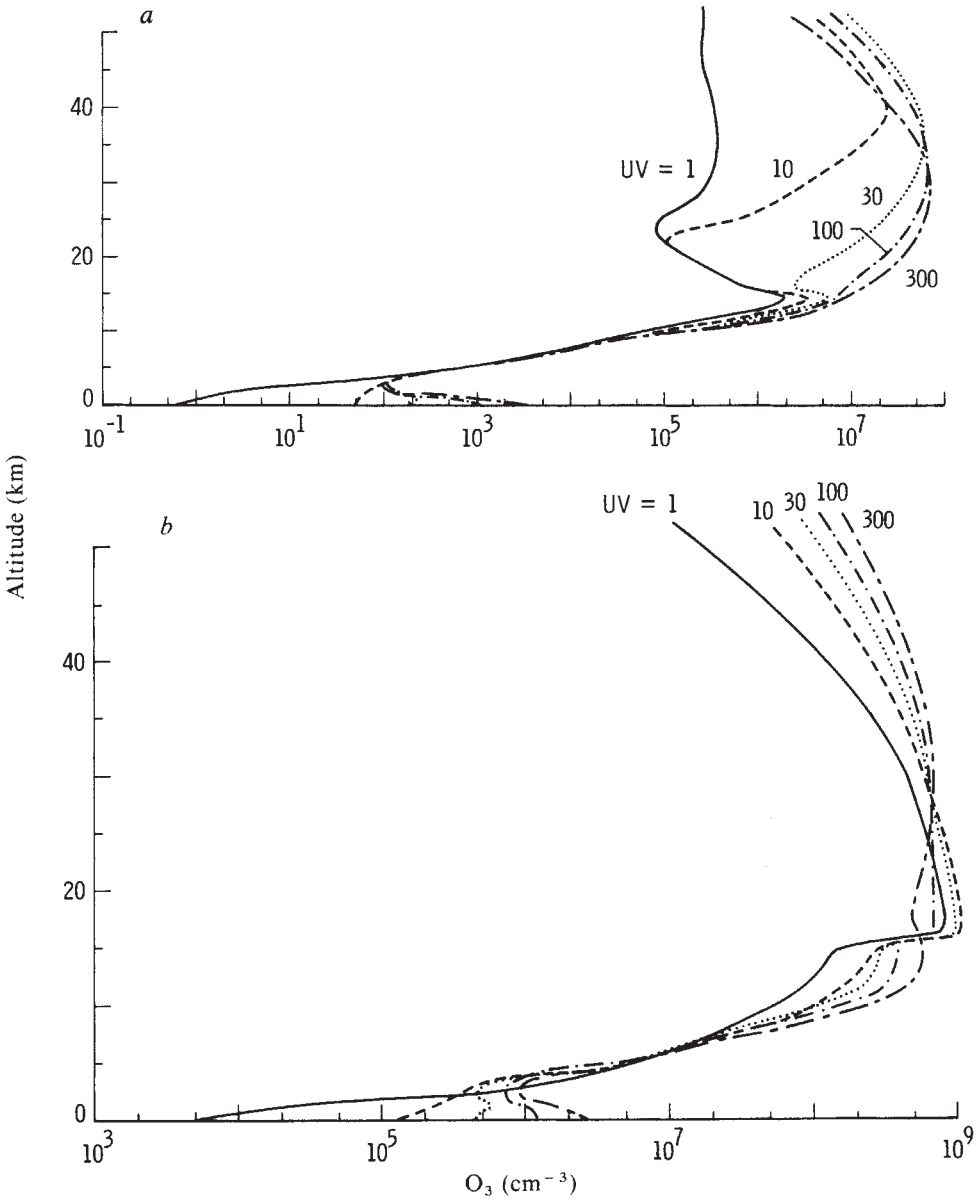

Fig. 2 Vertical distribution of O_3 in the prebiological palaeoatmosphere for levels of solar UV from 1 to 300 times the present value for a CO_2 level of: *a*, 280 p.p.m.v.; *b*, 28,000 p.p.m.v.

hydrogen burning and becomes stable, it emits about 100 times the UV radiation presently observed in the Sun.

There is no reason to believe that the youth of the Sun differed from that indicated by the T-Tauri and other young stars. We, therefore, conclude that the UV output of the young Sun was 10–1,000 times its present value. The high level of UV radiation thus indicated must have a profound effect on our understanding of the early atmosphere of the Earth.

Photochemistry of oxygen and ozone

Enhanced levels of UV radiation that may have been emitted from the Sun in its early stages may have had some very important implications for the origin and evolution of the early atmosphere, particularly for prebiological levels of oxygen (O_2) and ozone (O_3). In the prebiological palaeoatmosphere the formation of O_2 was initiated by solar UV radiation, that is, the photolysis of water vapour (H_2O), accompanied by the exospheric escape of atomic hydrogen (H), and the photolysis of carbon dioxide (CO_2). The photochemical reactions governing these processes are:

$$H_2O + h\nu \rightarrow OH + H;\ \lambda \leqslant 240\ \text{nm} \quad (1)$$

and,

$$CO_2 + h\nu \rightarrow CO + O;\ \lambda \leqslant 230\ \text{nm} \quad (2)$$

Table 3 Photodissociation reactions and diurnally-averaged rates at 53.5 km for a latitude of 30° (equinoctial conditions) (for present atmosphere)

No.	Reaction	Destruction ($cm^{-3}\ s^{-1}$)
J1	$O_2 + h\nu \rightarrow O + O$	1.41×10^{6}
J2	$O_3 + h\nu \rightarrow O + O_2$	4.40×10^{6}
J3	$O_3 + h\nu \rightarrow O(^1D) + O_2$	7.07×10^{7}
J4	$H_2O + h\nu \rightarrow OH + H$	5.32×10^{2}
J5	$N_2O + h\nu \rightarrow O(^1D) + N_2$	1.29×10^{2}
J6	$HNO_3 + h\nu \rightarrow OH + NO_2$	2.63×10^{0}
J7	$NO_2 + h\nu \rightarrow O + NO$	1.33×10^{4}
J8	$H_2O_2 + h\nu \rightarrow OH + OH$	2.52×10^{2}
J9	$HNO_2 + h\nu \rightarrow OH + NO$	4.31×10^{1}
J10	$NO_3 + h\nu \rightarrow NO + O_2$	7.85×10^{-1}
J11	$NO_3 + h\nu \rightarrow NO_2 + O$	7.85×10^{0}
J12	$N_2O_5 + h\nu \rightarrow NO_2 + NO_3$	5.21×10^{-4}
J13	$HCl + h\nu \rightarrow H + Cl$	1.47×10^{0}
J14	$ClO_2 + h\nu \rightarrow ClO + O$	6.41×10^{-3}
J15	$ClO + h\nu \rightarrow Cl + O$	1.45×10^{2}
J16	$Cl_2 + h\nu \rightarrow Cl + Cl$	1.43×10^{-6}
J17	$ClNO_3 + h\nu \rightarrow ClO + NO_2$	4.77×10^{-4}
J18	$CCl_4 + h\nu \rightarrow 2Cl + \text{products}$	1.27×10^{-5}
J19	$CH_3Cl + h\nu \rightarrow CH_3 + Cl$	1.09×10^{-2}
J20	$CH_2O + h\nu \rightarrow H + HCO$	4.00×10^{1}
J21	$CH_2O + h\nu \rightarrow H_2 + CO$	4.15×10^{1}
J22	$CH_3CCl_3 + h\nu \rightarrow Cl + \text{products}$	1.20×10^{-5}
J23	$CH_3OOH + h\nu \rightarrow CH_3O + OH$	1.82×10^{0}
J24	$NO + h\nu \rightarrow N + O$	9.12×10^{1}
J25	$CO_2 + h\nu \rightarrow CO + O$	4.51×10^{-1}

Table 4 Chemical reactions

No.	Reaction	Rate constant ($cm^3\ s^{-1}$ or $cm^6\ s^{-1}$)
1	$O+O_2+M\rightarrow O_3+M$	$1.1\times10^{-34}\exp(510/T)$
2	$O+O_3\rightarrow 2O_2$	$1.5\times10^{-11}\exp(-2{,}218/T)$
3	$O(^1D)+O_2\rightarrow O+O_2$	$3.2\times10^{-11}\exp(67/T)$
4	$O(^1D)+N_2\rightarrow O+N_2$	$1.8\times10^{-11}\exp(107/T)$
5	$N_2O+O(^1D)\rightarrow 2NO$	6.6×10^{-11}
6	$N_2O+O(^1D)\rightarrow N_2+O_2$	5.1×10^{-11}
7	$NO+O+M\rightarrow NO_2+M$	$1.6\times10^{-32}\exp(584/T)$
8	$NO+O_3\rightarrow NO_2+O_2$	$2.3\times10^{-12}\exp(-1{,}450/T)$
9	$NO_2+O\rightarrow O_2+NO$	9.3×10^{-12}
10	$NO_2+O_3\rightarrow NO_3+O_2$	$1.2\times10^{-13}\exp(-2{,}450/T)$
11	$NO+HO_2\rightarrow NO_2+OH$	$3.5\times10^{-12}\exp(250/T)$
12	$NO_2+OH+M\rightarrow HNO_3+M$	*
13	$HNO_3+OH\rightarrow NO_3+H_2O$	$1.5\times10^{-14}\exp(650/T)$
14	$H_2O+O(^1D)\rightarrow 2OH$	2.2×10^{-10}
15	$H+O_2+M\rightarrow HO_2+M$	$2.1\times10^{-32}\exp(290/T)$
16	$H+O_3\rightarrow OH+O_2$	$1.4\times10^{-10}\exp(-470/T)$
17	$OH+O\rightarrow H+O_2$	$2.3\times10^{-11}\exp(110/T)$
18	$OH+O_3\rightarrow HO_2+O_2$	$1.6\times10^{-12}\exp(-940/T)$
19	$OH+OH\rightarrow H_2O+O$	$4.5\times10^{-12}\exp(-275/T)$
20	$HO_2+O\rightarrow OH+O_2$	4.0×10^{-11}
21	$HO_2+O_3\rightarrow OH+2O_2$	$1.1\times10^{-14}\exp(-580/T)$
22	$HO_2+OH\rightarrow H_2O+O_2$	4.0×10^{-11}
23	$HO_2+HO_2\rightarrow H_2O_2+O_2$	2.5×10^{-12}
24	$H_2O_2+OH\rightarrow HO_2+H_2O$	$2.7\times10^{-12}\exp(-145/T)$
25	$OH+NO+M\rightarrow HNO_2+M$	*
26	$NO+NO_3\rightarrow 2NO_2$	2.0×10^{-11}
27	$O(^1D)+N_2+M\rightarrow N_2O+M$	3.5×10^{-37}
28	$O(^1D)+H_2\rightarrow OH+H$	9.9×10^{-11}
29	$O(^1D)+CH_4\rightarrow OH+CH_3$	1.4×10^{-10}
30	$NO_2+O+M\rightarrow NO_3+M$	1.0×10^{-31}
31	$NO_2+NO_3\rightarrow N_2O_5$	$1.5\times10^{-13}\exp(861/T)$
32	$N_2O_5\rightarrow NO_2+NO_3$	$1.2\times10^{14}\exp(-10{,}319/T)$
33	$N_2O_5+H_2O\rightarrow 2HNO_3$	1.0×10^{-20}
34	$N_2O_5+O\rightarrow 2NO_2+O_2$	3.0×10^{-16}
35	$N+NO_2\rightarrow N_2O+O$	$2.1\times10^{-11}\exp(-800/T)$
36	$N+O_2\rightarrow NO+O$	$4.4\times10^{-12}\exp(-3{,}220/T)$
37	$N+NO\rightarrow N_2+O$	3.4×10^{-11}
38	$N+O_3\rightarrow NO+O_2$	1.0×10^{-15}
39	$Cl+O_3\rightarrow ClO+O_2$	$2.8\times10^{-11}\exp(-257/T)$
40	$ClO+O\rightarrow Cl+O_2$	$7.7\times10^{-11}\exp(-130/T)$
41	$ClO+NO\rightarrow Cl+NO_2$	$6.5\times10^{-12}\exp(280/T)$
42	$Cl+CH_4\rightarrow HCl+CH_3$	$9.6\times10^{-12}\exp(-1{,}350/T)$
43	$Cl+H_2\rightarrow HCl+H$	$3.5\times10^{-11}\exp(-2{,}290/T)$
44	$Cl+HO_2\rightarrow HCl+O_2$	4.8×10^{-11}
45	$Cl+H_2O_2\rightarrow HCl+HO_2$	$1.1\times10^{-12}\exp(-980/T)$
46	$Cl+HNO_3\rightarrow HCl+NO_3$	$1.0\times10^{-11}\exp(-2{,}170/T)$
47	$Cl+CH_2O\rightarrow HCl+HCO$	$9.2\times10^{-11}\exp(-68/T)$
48	$HCl+OH\rightarrow Cl+H_2O$	$2.8\times10^{-12}\exp(-425/T)$
49	$HCl+O\rightarrow Cl+OH$	$1.1\times10^{-11}\exp(-3{,}370/T)$
50	$Cl+O_2+M\rightarrow ClO_2+M$	*
51	$ClO_2+M\rightarrow Cl+O_2+M$	$2.7\times10^{-9}\exp(-2{,}650/T)$
52	$Cl+ClO_2\rightarrow 2ClO$	8.0×10^{-12}
53	$Cl+ClO_2\rightarrow Cl_2+O_2$	1.4×10^{-10}
54	$OH+OH+M\rightarrow H_2O_2+M$	*
55	$H_2O_2+O\rightarrow OH+HO_2$	$2.8\times10^{-12}\exp(-2{,}125/T)$
56	$OH+CH_4\rightarrow CH_3+H_2O$	$2.4\times10^{-12}\exp(-1{,}710/T)$
57	$ClO+NO_2+M\rightarrow ClNO_3+M$	*
58	$O+ClNO_3\rightarrow ClO+NO_3$	$3.0\times10^{-12}\exp(808/T)$
59	$O(^1D)+HCl\rightarrow OH+Cl$	1.4×10^{-10}
60	$H_2+OH\rightarrow H_2O+H$	$1.2\times10^{-11}\exp(-2{,}200/T)$
61	$CH_3+O_2+M\rightarrow CH_3O_2+M$	*
62	$CH_3O_2+HO_2\rightarrow CH_3OOH+O_2$	$7.7\times10^{14}\exp(1{,}300/T)$
63	$CH_3O_2+NO\rightarrow CH_3O+NO_2$	7.4×10^{-12}
64	$CH_3O+O_2\rightarrow CH_2O+HO_2$	$9.2\times10^{-13}\exp(-2{,}200/T)$
65	$CH_2O+OH\rightarrow HCO+H_2O$	1.0×10^{-11}
66	$CH_2O\rightarrow OH+HCO$	$3.0\times10^{-11}\exp(-1{,}550/T)$
67	$HCO+O_2\rightarrow CO+HO_2$	5.0×10^{-12}
68	$CO+OH\rightarrow H+CO_2$	*
69	$CH_3Cl+OH\rightarrow Cl+$products	$1.8\times10^{-12}\exp(-1{,}112/T)$
70	$CH_3OOH+OH\rightarrow CH_3O_2+H_2O$	$2.1\times10^{-12}\exp(-145/T)$
71	$OH+CH_3CCl_3\rightarrow Cl+$products	$5.4\times10^{-12}\exp(-1{,}820/T)$
72	$O+O+M\rightarrow O_2+M$	$2.8\times10^{-34}\exp(710/T)$
73	$H+H+M\rightarrow H_2+M$	8.3×10^{-33}
74	$H_2+O\rightarrow OH+H$	$3.0\times10^{-14}\exp(-4{,}480/T)$
75	$H+HO_2\rightarrow O_2+H_2$	4.7×10^{-11} (×0.29)
76	$H+HO_2\rightarrow H_2O+O$	4.7×10^{-11} (×0.02)
77	$H+HO_2\rightarrow OH+OH$	4.7×10^{-11} (×0.69)

* See ref. 34.

Reaction (1) leads to the production of oxygen atoms (O) through:

$$OH+OH\rightarrow O+H_2O \quad (3)$$

The oxygen atoms formed in reactions (2) and (3) form molecular oxygen (O_2) through the following reactions:

$$O+O+M\rightarrow O_2+M \quad (4)$$

$$O+OH\rightarrow O_2+H \quad (5)$$

The destruction of O_2 is controlled by its photolysis and reaction with molecular hydrogen (H_2) resulting from volcanic emissions:

$$O_2+h\nu\rightarrow O+O;\ \lambda\leq 242\ nm \quad (6)$$

and

$$2H_2+O_2\rightarrow 2H_2O \quad (7)$$

(See reactions (19) and (74) in Table 4.)
Closely coupled to the origin and evolution of O_2 is the origin and evolution of O_3. O_3 is photochemically produced through the reaction:

$$O+O_2+M\rightarrow O_3+M \quad (8)$$

Table 5 Column density of O_3 in the prebiological palaeoatmosphere for various combinations of atmospheric CO_2 and solar UV flux

Solar UV flux	CO_2	O_3 column (cm^{-2})
1*	1†	1.72×10^{12}
	10	2.49×10^{14}
	100	1.38×10^{15}
10	1	3.94×10^{13}
	10	5.36×10^{14}
	100	1.95×10^{15}
30	1	1.50×10^{14}
	10	7.81×10^{14}
	100	2.06×10^{15}
100	1	1.76×10^{14}
	10	8.15×10^{14}
	100	2.04×10^{15}
300	1	1.52×10^{12}
	10	9.41×10^{14}
	100	2.19×10^{15}

* Present value of solar UV flux[27]. Other values represent multiples of present value.
† Pre-industrial level of CO_2 (p.p.m.v.). Other values represent multiples of this value.

O_3 is photochemically destroyed through photolysis and reaction with O:

$$O_3+h\nu\rightarrow O_2+O;\ \lambda\leq 1{,}100\ nm \quad (9)$$

and

$$O_3+O\rightarrow 2O_2 \quad (10)$$

In addition, O_3 is photochemically destroyed by a series of catalytic cycles involving the oxides of nitrogen ($NO+NO_2$), hydrogen ($OH+HO_2$), and chlorine ($Cl+ClO$).

To study the effects of enhanced solar UV radiation on the levels of O_2 and O_3 in the prebiological palaeoatmosphere, the photochemical model of the palaeoatmosphere of Levine *et al.*[24] was modified. This model which was originally developed to study the effect of anthropogenic perturbations on future

levels of O_3, has been used to study the origin and evolution of O_3 for specified levels of palaeoatmospheric O_2 ranging from 10^{-4} of the present atmospheric level (PAL) to the present atmospheric level (1 PAL)[24]. The model was modified such that O_2, CO_2, and H_2 which were previously specified as input parameters are now considered as chemically-active species, whose vertical profiles are calculated using coupled species continuity–flux equations, which contain both chemical production and loss terms and vertical eddy transport[25]. The inclusion of O_2, CO_2, and H_2 as chemically-active species makes it a total of 31 species whose vertical profiles are solved simultaneously by coupled species continuity–flux equations. The other calculated species are: O_3, O, N_2O, N, NO, NO_2, NO_3, N_2O_5, HNO_2, HNO_3, H_2O, H, OH, HO_2, H_2O_2, CH_4, CO, CH_3OOH, CH_2O, CH_3, HCO, CH_3O_2, CH_3O, Cl, ClO, HCl, CH_3Cl, and $ClNO_3$. Very short-lived species assumed to be in instantaneous photochemical equilibrium include: $O(^1D)$, ClO_2, and Cl_2. The model now includes 25 photochemical processes listed in Table 3, and 77 chemical reactions listed in Table 4. The US Standard Atmospheric Mid-Latitude Spring/Autumn temperature and H_2O profiles are specified in the troposphere. A primordial temperature profile that decreases linearly from the tropopause to the mesosphere is used. This profile is based on coupled photochemical–radiative equilibrium temperature calculations in the O_3-deficient palaeoatmosphere[26]. While H_2O is specified in the troposphere, it is calculated through the continuity–flux equation for H_2O in the stratosphere. Water soluble species, for example, HNO_3, H_2O_2, CH_3OOH, HCl, ClO, and $ClNO_3$ are lost throughout rainout, with a rainout coefficient of $1.0\times10^{-6}\,s^{-1}$. The model extends from the surface up to 53.5 km with the tropopause at a height of 14.5 km. Photodissociation rates are diurnally-averaged for a latitude of 30° and solar declination of 0°. The model includes the solar spectrum from 110 to 735 nm (ref. 27). Further details about the model are given in refs 24, 25.

For the present calculations, we have incorporated the boundary conditions for O_2 and H_2 given in ref. 28. O_2 is considered as a chemically-active species with a zero flux lower boundary condition and H_2 has a prescribed surface mixing ratio of 17 p.p.m.v. (ref. 28). We have studied the sensitivity of prebiological O_2 and O_3 to the level of CO_2 by performing calculations for the pre-industrial CO_2 value (280 p.p.m.v.), and for 10–100 times this value. Volatile outgassing scenarios suggest that the early atmosphere may have contained as much as three orders of magnitude more CO_2 than found in the present atmosphere[29,30]. According to these scenarios, the bulk of the early CO_2 went into the ocean and eventually formed sedimentary carbonates. The outgassed CO_2 on both Mars and Venus had a very different fate—remaining in the atmosphere–presumably due to the lack of liquid water and life on these planets. For our calculations we have used five values for the flux of solar UV: the present value[27] and multiples of 10, 30, 100, and 300 times the present value.

Oxygen and ozone in the prebiological palaeoatmosphere

O_2 profiles for the pre-industrial level of CO_2 (280 p.p.m.v.) and 100 times this value are given in Fig. 1. For each CO_2 level calculations have been performed for five values of solar UV radiation ranging from 1 to 300 times the present value. The calculated O_2 profile for contemporary values of CO_2 and UV exhibits a very strong altitude dependence, with a minimum O_2 mixing ratio of $<10^{-14}$ at the surface and a maximum O_2 mixing ratio of about 2×10^{-6} above 40 km, in excellent agreement with earlier calculations[28]. For a CO_2 value of 280 p.p.m.v. (Fig. 1), we found that increasing the UV flux from the present value to 300 times the present value resulted in increasing the surface mixing ratio of O_2 from $<10^{-14}$ to $\sim10^{-11}$. The O_2 maximum between 40 and 50 km increased from a mixing ratio of $\sim2\times10^{-6}$ to 8×10^{-5} as the solar UV flux was increased by a factor of 300. For a CO_2 value of 100 times the pre-industrial value (Fig. 1*b*), increasing the UV flux by a factor of 300 increased the surface mixing ratio of O_2 from 10^{-12} to 10^{-9}, and increased the O_2 maximum at ~50 km from $\sim3\times10^{-5}$ to $\sim2\times10^{-3}$. The corresponding O_3 calculations are shown in Fig. 2*a* (for CO_2 = 280 p.p.m.) and Fig. 2*b* (for CO_2 = 100 times greater). For a CO_2 value of 280 p.p.m.v. (Fig. 2*a*), increasing the UV flux by a factor of 300 increased the surface concentration of O_3 from 1 to $\sim3\times10^3\,cm^{-3}$ and increased both the height of the O_3 maximum from 14.5 to ~30 km and the peak concentration from 1×10^6 to $\sim5\times10^7\,cm^{-3}$. For the enhanced value of CO_2 (Fig. 2*b*), increasing the UV flux by a factor of 300 increased the surface concentration of O_3 from 5×10^3 to $2\times10^6\,cm^{-3}$. For this level of CO_2 and for all values of enhanced UV radiation the height of O_3 maximum was found to be between 15 and 20 km with a concentration that varied between 5 and $10\times10^8\,cm^{-3}$. The total O_3 column (molecules cm^{-2}) above the surface of the Earth for the O_3 profiles shown in Fig. 2 and for a CO_2 value of 10 times the pre-industrial value is summarized in Table 5.

Conclusion

Our calculation indicates that the surface mixing ratio of O_2 increased by a factor of 10^4–10^6 times the standard value of 10^{-15} (depending on the assumed value of CO_2) for enhanced level of UV radiation associated with the early Sun. Corresponding enhancement of O_3 level was also found.

These increased levels of O_2 and O_3 may have had important implications for early geology and on the origin and evolution of life. While the details of such implications are beyond the scope of this article, note that the higher value of O_2 found here falls within the lower (10^{-13}) and upper (10^{-3}) O_2 values arrived at to explain the simultaneous existence of oxidized iron and reduced uranium on the early Earth[31–33].

V.M.C. and J.S.L. thank Dr K. M. Towe for his helpful suggestions. C.L.I. thanks Dr M. S. Giampapa for assistance.

Received 28 December 1981; accepted 23 February 1982.

1. Newman, M. J. & Rood, R. T. *Science* **198,** 1035 (1977).
2. Sagan, C. & Mullen, G. *Science* **177,** 52 (1972).
3. Sagan, C. *Science* **269,** 224 (1977).
4. Owen, T., Cess, R. D. & Ramanathan, V. *Nature* **277,** 640 (1979).
5. Henderson-Sellers, A. & Meadows, A. J. *Nature* **270,** 589 (1977).
6. Berkner, L. V. & Marshall, L. C. *J. atmos. Sci.* **22,** 225 (1965).
7. Ratner, M. I. & Walker, J. C. G. *J. atmos. Sci.* **29,** 803 (1972).
8. Blake, A. J. & Carver, H. J. *J. atmos. Sci* **34,** 720 (1977).
9. Levine, J. S., Hays, P. B. & Walker, J. C.G. *Icarus* **39,** 295 (1979).
10. Kasting, J. F. & Donahue, T. M. *J. geophys. Res.* **85,** 3255 (1980).
11. Levine, J. S., Boughner, R. E. & Smith, K. A. *Origins of Life* **10,** 199 (1980).
12. Levine, J. S. *Origins of Life* **10,** 313 (1980).
13. Appenzeller, I., Chavarria, C., Krautter, J, Mundt, R. & Wolf, B. *Astr. Astrophys.* **90,** 184 (1980).
14. Appenzeller, I. & Wolf, B. *Astr. Astrophys.* **75,** 164 (1979).
15. Brown, A., Jordan, C., Millar, T. J., Gondhaekar, P. & Wilson, R. *Nature* **290,** 34 (1981).
16. Gahm, G. F., Kredga, K., Liseau, R. & Dravns, D. *Astr. Astrophys.* **73,** L4 (1979).
17. Gondhalekar, P., Penston, M. V. & Wilson, R. *The First Year of IUE* (ed. Willis, A. J.) 109 (University College, London, 1979).
18. Imhoff, C. L. & Giampapa, M. S. *Astrophys. J. Lett.* **239,** L115 (1980); in *The Universe at Ultraviolet Wavelengths: The First Two Years of IUE* (ed. Chapman, R. D.) 185 (NASA Conf. Publ. 2171, 1981); in *Proc. 2ndCambridge Workshop on Cool Stars, Stellar Systems and the Sun* (ed. Giampapa, M. S.) (SAO Spec. Rep., in the press).
19. Cohen, M. & Kuhi, L. V. *Astrophys. Suppl.* **41,** 743 (1979).
20. Boesgaard, A. M. & Simon, T. in *Proc. 2nd Cambridge Workshop on Cool Stars, Stellar Systems and the Sun* (ed. Giampapa, M. S.) (SAO Spec. Rep., in the press).
21. Wilson, O. C. *Astrophys. J.* **138,** 832 (1963).
22. Wilson, O. C. & Skumanich, A. *Astrophys. J.* **140,** 1401 (1964).
23. Skumanich, A. *Astrophys. J.* **171,** 565 (1972).
24. Levine, J. S., Augustsson, T. R., Boughner, R. E., Natarajan, M. & Sacks, L. J. in *Comets and the Origin of Life* (ed. Ponnamperuma, C.) 161 (Reidel, Dordrecht, 1981).
25. Levine, J. S., Augustsson, T. R. & Natarajan, M. *Origins of Life* **12** (in the press).
26. Levine, J. S. & Boughner, R. E. *Icarus* **39,** 310 (1979).
27. Ackermann, M. in *Mesospheric Models and Related Experiments* (ed. Fiocco, G.) 149 (Reidel, Dordrecht, 1971).
28. Kasting, J. F. & Walker, J. C. G. *J. geophys. Res.* **86,** 1147 (1981).
29. Hart, M. H. *Icarus* **38,** 23 (1978).
30. Levine, J. S. in *Comparative Planetology* (ed. Ponnamperuma, C.) 165 (Academic, New York, 1978).
31. Kline, C. & Bricker, O. P. *Econ. Geol.* **72,** 1457 (1977).
32. Grandstaff, D. E. *Precamb. Res.* **13,** 1 (1980).
33. Towe, K. M. *Nature* **274,** 657 (1978).
34. *Chemical Kinetic and Photochemical Data for Use in Stratospheric Modelling* JPL Publ. 81-3 (Jet Propulsion Laboratory, Pasadena, 1981).